

1 **SIBERIAN PINE DECLINE AND MORTALITY IN SOUTHERN SIBERIAN**
2 **MOUNTAINS**

3 V.I. Kharuk^{1§}, S.T. Im¹, P.A. Oskorbin¹, I.A. Petrov¹, K.J. Ranson²

4 ¹V. N. Sukachev Institute of Forest and Siberian Federal University, Krasnoyarsk, Russia,
5 (kharuk@ksc.krasn.ru)

6
7 [§]Corresponding author

8 ²NASA's Goddard Space Flight Center, Greenbelt, MD 20771, USA

9
10 **Abstract**

11 The causes and resulting spatial patterns of Siberian pine mortality in eastern Kuznetzky
12 Alatau Mountains, Siberia were analyzed based on satellite (Landsat, MODIS) and
13 dendrochronology data. Climate variables studied included temperature, precipitation and
14 Standardized Precipitation-Evapotranspiration Index (SPEI) drought index. Landsat data analysis
15 showed that stand mortality was first detected in the year 2006 at an elevation of 650 m, and
16 extended up to 900 m by the year 2012. Mortality was accompanied by a decrease in MODIS-
17 derived vegetation index (EVI). The area of dead stands and the upper mortality line were
18 correlated with increased drought. The uphill margin of mortality was limited by elevational
19 precipitation gradients. Dead stands (i.e., >75% tree mortality) were located mainly on southern
20 slopes. With respect to slope, mortality was observed within a 7°-20° range with greatest
21 mortality occurring on convex terrain. Tree radial increment measurements correlate and were
22 synchronous with SPEI ($r^2=0.37$, $r_s=80$). Increasing synchrony between tree ring growth and
23 SPEI indicates that drought has reduced the ecological niche of Siberian pine. The results also
24 showed the primary role of drought stress on Siberian pine mortality. A secondary role may be
25 played by bark beetles and root fungi attacks.

26 The observed Siberian pine mortality is part of a broader phenomenon of “dark needle conifers”
27 (DNC, i.e., Siberian pine, fir and spruce) decline and mortality in European Russia, Siberia, and
28 the Russian Far East. All locations of DNC decline coincided with areas of observed drought
29 increase. The results obtained are one of the first observations of drought-induced decline and
30 mortality of DNC at the southern border of boreal forests. Meanwhile if model projections of
31 increased aridity are correct DNC, within the southern part of its range may be replaced by
32 drought-resistant *Pinus silvestris* and *Larix sibirica*.

33
34 **Keywords:** climate-induced tree mortality, drought impact on forests, tree die-off, Siberian pine
35 decline

36

37 **1. Introduction**

38

39 Forest decline and mortality caused by drought during the last decades has been documented
40 on every continent (Allen et al., 2009). Elevated temperatures and water stress has caused forest
41 mortality in Europe, including increased stand mortality in Spain (Penuelas et al., 2001), France
42 (Breda et al., 2006; Landmann and Dreyer, 2006), Switzerland and Italy (Bigler et al., 2006;
43 Dobbertin and Rigling, 2006). In North America *Populus tremuloides* mortality was observed
44 across a million hectares (Hogg et al., 2008; Worrall et al., 2010; Anderegg et al., 2012). In the
45 south-western part of USA drought-induced mortality of *Pinus edulis* was also documented for
46 an area of over a million hectares (Breshears et al., 2005; Raffa et al., 2008; Van Mantgem et al.,
47 2009). In Russia birch (*Betula pendula*) stands decline was recently described in the southeastern
48 Siberia forest-steppe (Kharuk et al., 2013).

49 Scenarios of climate changes are likely to include further increases in drying, frequency and
50 severity of droughts in some forested areas (Christensen et al., 2007; IPCC, 2007; Seager et al.,
51 2007; Sterl et al., 2008; Aitken et al., 2008). This may lead to reduced forests growth and
52 increases in stress and mortality caused by synergy of drought impact and climate-induced
53 changes in the dynamics of dendrophyl insects and fungi (Lucht et al., 2006; Scholze et al.,
54 2006; Lloyd and Bunn, 2007). Severe water stress is decreasing both growth and oleoresin
55 production, making trees more susceptible to bark beetle attack. In addition to water stress
56 affecting host tree susceptibility, insect population dynamics were directly affected by increasing
57 temperature (Hansen et al., 2001; Breshears et al., 2005).

58 In Russia decline and mortality of “dark needle conifers” (DNC: spruce (*Picea obovata*),
59 Siberian pine (*Pinus sibirica*), fir (*Abies sibirica*)) were reported from the western border (i.e.,
60 Kaliningrad region) to the Russian Far East. During the 21st century, climate-caused mortality
61 was described in official Russian reports as the third-ranked factor (following fire and pest
62 impacts) (Efremov et al., 2012). In Archangelsk in the European part of Russia spruce decline
63 was observed over an area >1.6 million ha with mortality on the territory >390 thousands ha
64 (Fig. 1 (site 1)). Other potential causes of forest mortality considered were over mature stands,
65 drought, root fungi and insect attacks (Chuprova, 2008; Sanitary, 2008). In the Russian Far East,
66 mortality was reported over the vast area of mixed spruce (*Picea ajansis*) and fir (*Abies*
67 *nephrolepis*) forests within the Sihote-Alin Ridge (Fig.1 (site 7)). Mortality was observed mainly
68 for the mature stands (Age =100-160 years), whereas regeneration was usually not damaged.
69 Decline and die-off of spruce-fir stands were considered to be caused by “unfavorable climatic
70 factors with fungi as a co-factor” (Man’ko et al., 1998). According to the Russian Forest Service,

71 Siberian pine and fir decline and mortality were observed in the southern Siberian Mountains
72 (Kuznetzky Alatau and Sayan Mountains) and in the Baikal Mountains (mixed fir and Siberian
73 pine stands) (Fig. 1 (Sites 2, 3, 4, 5)). In addition, birch mortality was documented in the Trans-
74 Baikal area (Kharuk et al., 2013 (Fig. 1 (site 6))).

75 The goal of this paper was spatial and temporal analysis of Siberian pine mortality within the
76 Kuznetzky Alatau Mountains, and analysis of potential causes of this phenomenon. We
77 considered the following hypotheses. 1. Siberian pine decline and mortality were caused by
78 drought. 2. Mortality pattern was dependent on relief features. The following questions were also
79 addressed: When did the Siberian pine decline and mortality begin? What were the causes of
80 stand mortality? What are the spatial and temporal patterns of mortality?

81

82 **2. Material and methods**

83

84 *2.1. Study area*

85

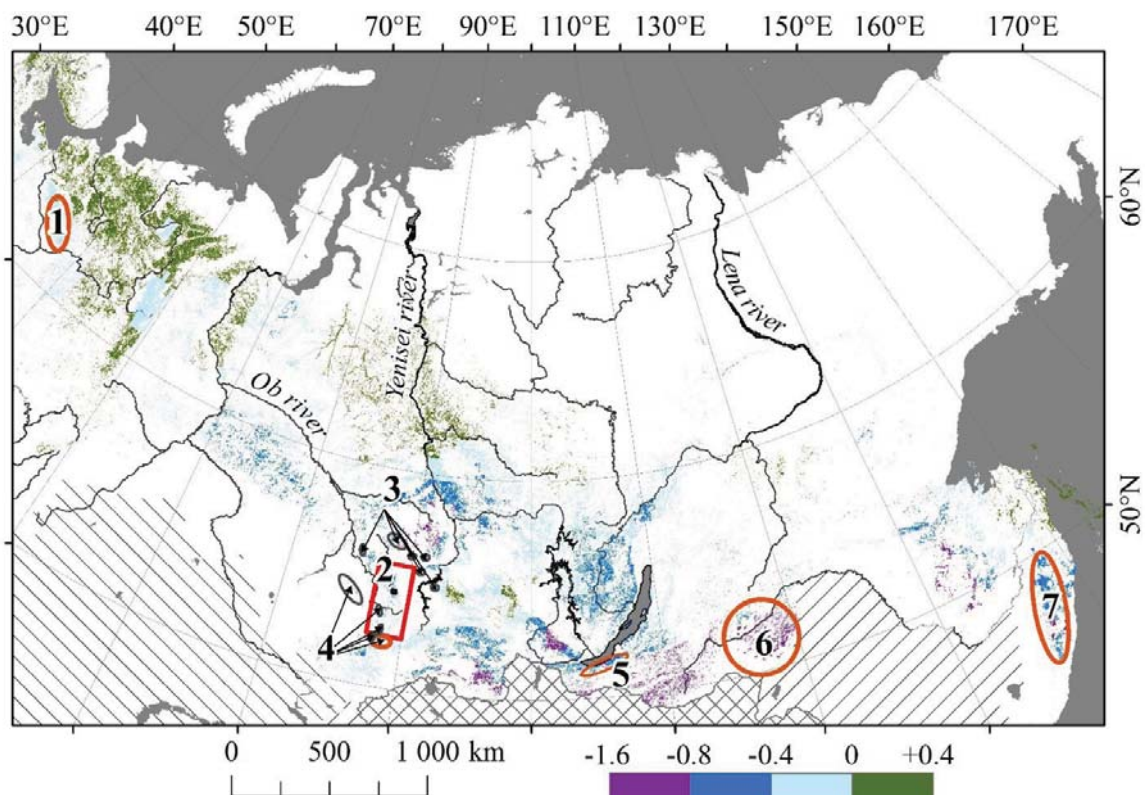
86 The study area (designated as the “Black Iyus” (BI) site) was located within the Kuznetzky
87 Alatau Mountains (Fig. 1). These mountains are part of the Sayan-Altai Mountains in southern
88 Siberia and composed of several northward oriented ridges with length and width about 300 km
89 and 150 km, respectively, and maximal height about 2200 m. These mountains have relatively
90 gentle slopes and are composed of limestone, quartzite, argillaceous and siliceous slates, with
91 multiple intrusions of granites, diorite, gabbro and tuff.

92

93 *2.2. Climate*

94

95 Monthly climate data for the area were obtained from KNMI Climate Explorer (Climate
96 Explorer, <http://climexp.knmi.nl>). Data were averaged for a cell size $0.5^{\circ} \times 0.5^{\circ}$. Climate within
97 the study area is continental with cold long winters and warm or hot summers. On western facing
98 slopes annual precipitation is about 600-800 mm (with >1500 mm) within the central windward
99 part of mountains). The western facing slopes actually create a "rain shadow" effect that results
100 in a decrease in precipitation on the eastern slopes, where annual precipitation were in the range
101 of 400-500 mm. Winter winds (predominately from the south-west) resulted in greatest
102 accumulation of snow on northern and eastern slopes. Climate data for the BI site are presented
103 in Table 1 and Fig. 2 (the beginning of the record is considered to be the year 1940 when reliable
104 meteorological observations started). According to this record, mean January and July
105 temperatures are -21.4°C and $+16^{\circ}\text{C}$, respectively.



106

107

108 Fig. 1. Location of forest stands decline and mortality in Siberia. Background: evergreen
 109 conifer map (Bartalev et al., 2011). Color scale: SPEI (Standard Precipitation Evaporation Index)
 110 anomaly (2000-2009 vs 1902-2009 yr.). Sites: 1 – spruce stands in Archangelsk region; 2 – DNC
 111 of Kuznetzky Alatau Mountains; 3, 4 – DNC stands in southern Siberia; 5 – fir and Siberian
 112 pine site in southern Baikal area; 6 – birch stands within Trans-Baikal area (Kharuk et al, 2013);
 113 (7) – spruce stands in Russian Far East (Man’ko et al, 1998).

113

114 Table 1. Climate data for the “Black Iyus” site.

Variable (1940-2009 yr)	Ann ual	Jun- Aug	Dec- Feb
Mean temperature, °C	-2.2	14.5	-20.0
Mean sum of precipitation, mm	562	234	71

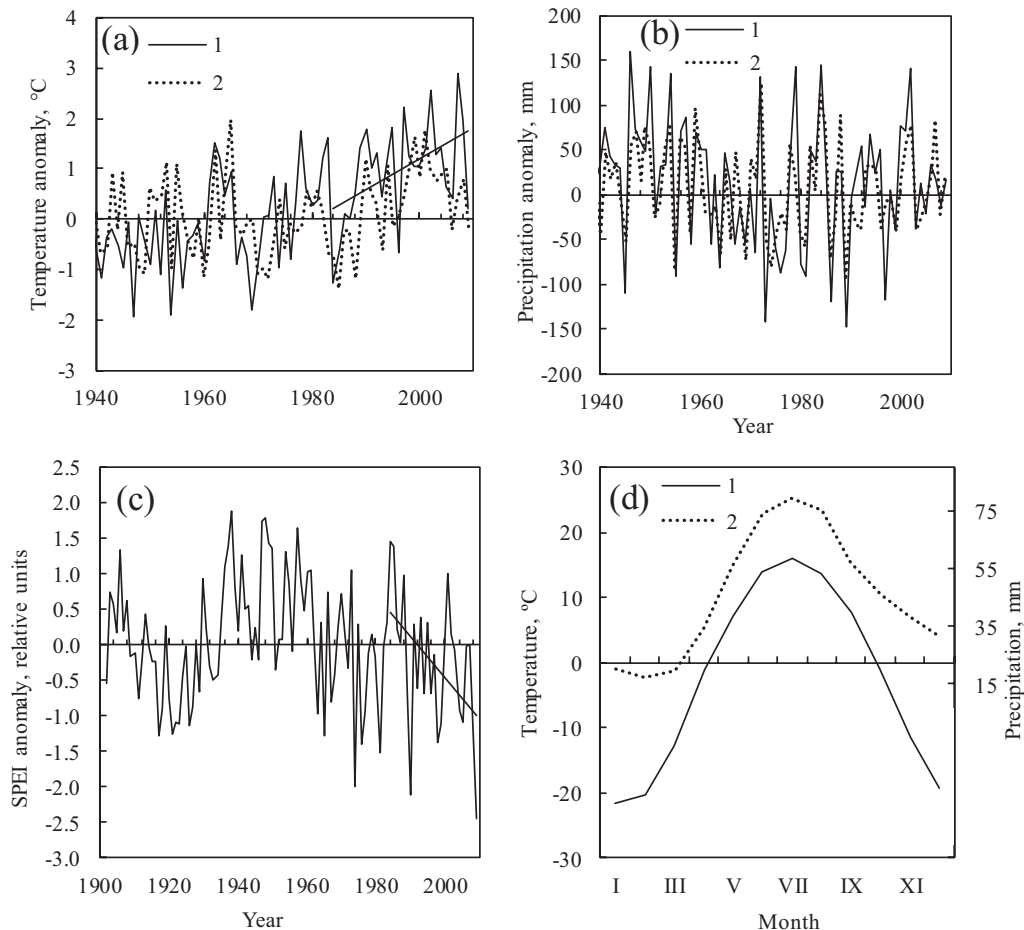
115

116 2.3. Vegetation

117

118 In Kuznetzky Mountains, tundra communities are typical at high elevations (1350-1500
 119 m.a.s.l.) with mountain-tundra soils. Within the subalpine belt (1100-1350 m) alpine meadows
 120 and sparse vegetation (*Betula tortuosa*, *Larix sibirica*, *Pinus sibirica* and *Abies sibirica*) grow on

121 mountain-subalpine soils. Top and middle parts of the forest belt (600-1100 m) are composed of
 122 Siberian pine dominated stands with an admixture of fir and spruce (*Picea obovata*). Soils are
 123 mountain light-grey rocky podzolized. Low elevations are occupied by larch and pine (*Pinus*
 124 *silvestris*) stands with admixture of Siberian pine and birch (*Betula pendula*). Here soils are
 125 mountain rocky podzolized. Steppes are found on steep south facing slopes at the lowest
 126 elevations (500-600 m.a.s.l.)



127
 128 Fig. 2. Climate variables within “Black Iyus” site. (a), (b) - mean air temperature and
 129 precipitation anomalies, correspondingly (1 – annual, 2 - May-August data); (c) – anomaly of
 130 SPEI drought index; (d) – annual (1) temperature and (2) precipitation. Trends for annual
 131 temperature (a) and SPIE (c) were significant at $p < 0.05$.

132

133 2.4. Field studies

134

135 Forest mortality within the BI site was reported by local foresters in the year 2006. Field studies
 136 were executed in the summer of 2012 and included forest type description, trees height and
 137 diameter measurements, canopy closure estimation, and cutting of tree disks for

138 dendrochronology analysis. The BI site is located within an area with elevations of about 640-
139 1040 m a.s.l. Stands are formed by Siberian pine (>95% of trees) with admixture of *Abies*
140 *sibirica* and *Picea obovata*. Canopy closure was about 0.8-0.9. Average tree height was about 30
141 m, and DBH was 28 cm. Stands were mature (mean age of trees was about 160 years; the
142 maximum Siberian pine lifetime is about 600-800 years). Ground cover was mesophytic (sedges
143 dominant). Litter thickness was about 3-5 cm. Soils were light-gray forest type underlined by
144 stony clay at 10-15 cm deepness. There were no signs of fires within study area, i.e., there were
145 no carbon and burnmarks on the boles. During the year of ground measurements logging was
146 carried out within areas of stands dieback and mortality. It is necessary to note that according to
147 Russian forest rules logging of Siberian pine stands is strictly prohibited except in decline or
148 dead stands. The area of logging within BI site is about 15 ha. Discs for dendrochronology
149 analysis were collected at about breast height.

150

151 2.5. *Dendrochronology analysis*

152

153 The dendrochronology dataset included 56 disks (24 from living trees, 11 from declining and
154 21 from dead trees). The surface of each disk was sanded, planed with a scalpel and treated with
155 a contrast enhancing powder. The widths of tree rings were measured with 0.01 mm precision
156 using a linear table instrument (LINTAB-III). The TSAP and COFECHA computer programs
157 were used in tree ring analysis and cross dating of chronology (Holmes, 1983; Rinn, 1996).
158 Dates of tree mortality were determined based on the master-chronology method (Fritts, 1991).
159 An initial master chronology was constructed based on 10 living trees. This master-chronology
160 was used for cross dating of the remaining samples. As soon as a given sample was dated, it was
161 included into the master chronology. This procedure provided increased reliability of further
162 analysis. The final master chronology included 39 individual tree-ring series. The mean
163 coefficient of correlation between individual tree-ring series and master-chronology was 0.43.
164 The mean sensitivity of individual series included into master-chronology was 0.173. Discs with
165 missing rings ($n = 8$) were not included into the master-chronology, but were involved in further
166 analysis. Discs which were not possible to cross-date ($n = 9$) were removed from further
167 analysis. Thus the final dataset ($n = 47$) was divided into “survivors” ($n = 15$) and “dead and
168 declining” ($n = 32$) groups. This division was based on radial increment trends during the last
169 decade (2000-2011) as described.

170 Trees with positive tree ring increments formed a “survivors group”, whereas a second group
171 contained trees with negative increment trend and dead trees. For both groups standard and
172 residual chronologies were constructed. Standard chronologies were indexed using ARSTAN

173 software (i.e., double detrending to remove long-term trends by negative exponential curve and a
 174 linear regression; Cook and Holmes, 1986). The resulting chronologies were a unitless index of
 175 radial tree growth. The residual chronologies were constructed based on standard chronologies
 176 by elimination of autocorrelation, i.e., increasing a climate signal (Cook and Holmes, 1986).
 177 Statistical analysis was carried out using Excel and StatSoft software; Student's *t*-test was used to
 178 estimate result significance (StatSoft Inc, 2013). In addition to the correlation coefficient (*r*), the
 179 coefficient of synchronization (*r_s*) was determined. The latter was calculated as the ratio of the
 180 number of annual segments with the same direction (i.e., increasing or decreasing growth
 181 increment) to the total segment number (Shiyatov, 1986).

182

183 2.6. Satellite data

184

185 2.6.1. Aqua/MODIS and Terra/MODIS data analysis

186

187 Aqua/MODIS and Terra/MODIS satellite data were used for temporal analysis of stands
 188 vigor based on Enhanced Vegetation Index (EVI). EVI is responsive to canopy structural
 189 variations, including leaf area index, stands vigor, canopy type, plant physiognomy, and canopy
 190 architecture (Huete et al., 1999). Technically EVI data are available as a ready to use MODIS
 191 product MOD13Q1 from NASA's site (EOSDIS, <http://reverb.echo.nasa.gov>). For this purpose a
 192 temporal series of satellite data from MODIS products were compiled.

193 EVI is defined as:

$$194 \quad EVI = G \times (\rho_{NIR} - \rho_{red}) \times (\rho_{NIR} - C_1 \times \rho_{red} + C_2 \times \rho_{blue} + L)^{-1}$$

195 where ρ_{NIR} , ρ_{red} and ρ_{blue} are atmospherically-corrected surface reflectance in MODIS bands #1
 196 (620-670 nm), #2 (841-876 nm) and #3 (459-479 nm); *L* is the canopy background adjustment;
 197 *C*₁ and *C*₂ are the coefficients of the aerosol correction; *G* – gain factor (Huete et al., 1999).

198 In this study the MODIS EVI values covered the period from 2000 to 2012 with ground
 199 resolution of 250×250 m. Earlier it was reported that Terra/MODIS sensor degradation impacted
 200 NDVI trend analysis (Wang et al., 2012). Here Terra/MODIS data were used for the 2000-2001
 201 period only, when there was no significant sensor degradation. The time interval 2002-2012 was
 202 analyzed based on Aqua/MODIS data which were already corrected (Wang et al., 2012).

203 A mask of evergreen conifers for the whole of Siberia and the study area in particular was
 204 generated based on the Terra Norte forest vegetation map (Bartalev et al., 2011). This mask was
 205 used to track changes within evergreen conifer stands only.

206

207 2.6.2. Landsat data and GIS analysis

208

209 Landsat scenes (MSS/TM/ETM+, 15-60 m spatial resolution, acquired during the years
 210 1976-2012) were obtained from USGS GloVis (<http://glovis.usgs.gov>). The selected scenes were
 211 georeferenced to topographic maps (scale 1:100000). Dead stands (i.e., those exhibiting >75%
 212 tree mortality) were visually detectable on the images. The total area of the analyzed territory
 213 was 382 ha. An analysis of the scenes showed that stand mortality could be detected as early as
 214 the year 2006. Also available were digitized maps of dead stands produced by a forestry expert
 215 for each year from 2006 to 2012. Image interpretation was facilitated by data acquired from our
 216 field studies. Polygons were delineated on an image display and recorded by ArcGIS software
 217 (<http://www.esri.com>).

218 Topography analysis of stand mortality was based on the DLR SRTM-X DEM product
 219 (<http://eoweb.dlr.de:8080/index.html>). DEM horizontal accuracy was ± 20 m (absolute) and
 220 ± 15 m (relative). The vertical accuracy was ± 16 m (absolute) and ± 6 m (relative). The minimum
 221 interval (contour) of elevation of 50 m was used. The following parameters were considered:
 222 elevation, aspect, slope steepness, and curvature (i.e., convex/concave slope parameters). Aspect,
 223 slope steepness and curvature data were calculated from SRTM-X DEM using ArcGIS tools.
 224 The aspect data were quantized into eight directions (i.e., by 45 degrees corresponding to north,
 225 northeast, east etc.). The distribution of landscape elements with given altitude, azimuth and
 226 slope steepness was uneven within the analyzed area and thus could lead to biased analysis. To
 227 avoid this, the data were normalized by the following procedure. The analyzed study area (about
 228 400 ha) with given azimuth, slope steepness and elevation was related to the larger (“reference”)
 229 territory (ca 3000 ha) with similar parameters:

$$230 \quad \kappa_{c(i)} = A_{c(i)-f} / A_{c(i)-I} \quad (1)$$

231 where the $c(i)$ subscript represents the i^{th} category of landscape feature c , $A_{c(i)-f}$ is the area of
 232 the given on-ground class within the i^{th} category of the topography feature c , and $A_{c(i)-I}$ is the area
 233 of the i^{th} category of topography feature c over the “reference” territory. ERDAS Imagine
 234 software (<http://geospatial.intergraph.com>) was used in the analysis.

235

236 2.7. *Water balance estimation*

237 For water balance estimation, the Standardized Precipitation-Evapotranspiration index (SPEI;
 238 Vicente-Serrano et al., 2010) was used. Like the PDSI (The Palmer Drought Severity Index;

239 Palmer, 1965), the SPEI measures drought severity according to intensity and duration, and can be used
 240 to identify the onset and end of drought episodes. The SPEI uses the monthly difference (D_i)
 241 between precipitation and PET (potential evapotranspiration):

$$242 \quad D_i = P_i - PET_i$$

243 PET (mm) is obtained by:

$$244 \quad PET = 16 \times K \times (10 \times T \times I^{-1})^m,$$

245 where T is the monthly mean temperature in °C; I is a heat index, which is calculated as the sum
 246 of 12 monthly index values, m is a coefficient depending on I , and K is a correction coefficient
 247 computed as a function of the latitude and month which takes into account number of sun hours
 248 in a day. SPEI data for the study area were calculated for the May-August period. May was
 249 added to summer period because May droughts were typical for the study area. Spatial resolution
 250 for the SPEI data was $0.5^\circ \times 0.5^\circ$ ($\sim 33 \times 56 \text{ km}^2$).

251

252 **3. Results**

253

254 *3.1. Remotely sensed data*

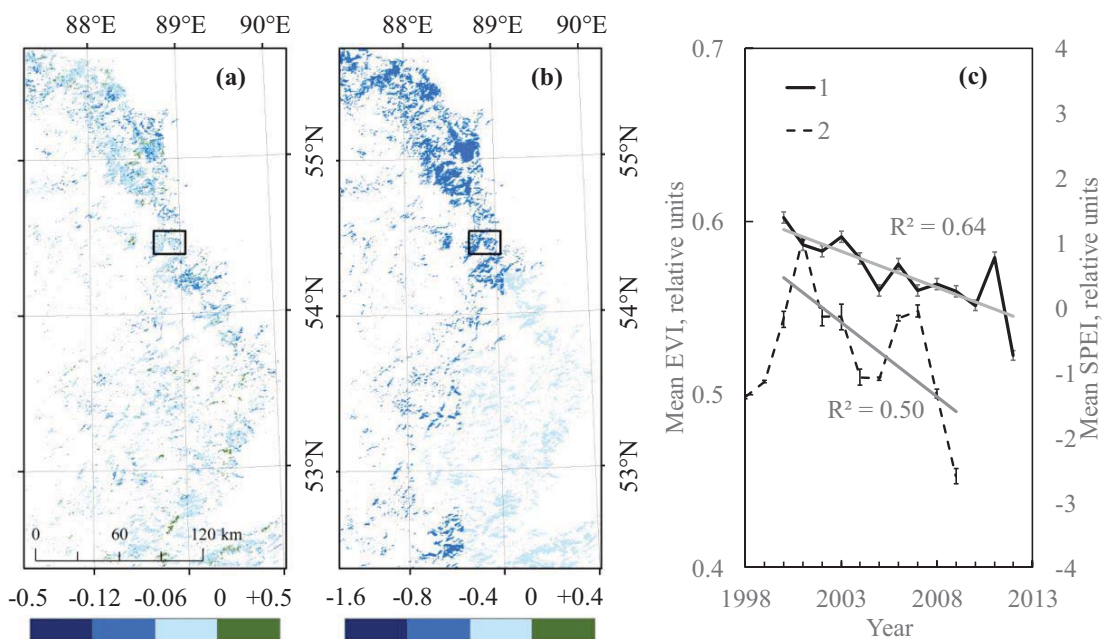
255

256 An overall decrease in Vegetation index (EVI) for “dark needle conifers” stands was
 257 observed within the Kuznetzky Alatau Mountains. This decrease in "greenness" was correlated
 258 with drought during the first decade of the 21st century (Fig. 3a, b). Within the BI site EVI
 259 decreased about ~4% ($p < 0.05$) between 2006 and 2012, and was accompanied with a drought
 260 increase (Fig. 3c). The dynamics of forest mortality are presented on Fig. 4, 5. With an increase
 261 in drought (i.e., SPEI decrease) the dead stands area increased ($r_1^2 = -0.98$) and stand mortality
 262 was propagated along the elevation gradient ($r_2^2 = -0.92$) (Fig. 5).

263

264 *3.2. Relief features*

265 Maximum mortality was observed on the slopes of southern and southeastern exposures (Fig.
 266 6b). The location of dead stands was relatively higher within convex terrain elements (Fig. 5c).
 267 With respect to slope, mortality was maximal within the range of slopes between 7° and 20° (>
 268 75% mortality; Fig. 6c). With respect to elevation, mortality was observed mainly within the
 269 lower elevation belt (starting from Black Iyus river level: 650 m a.s.l.) and decreasing upwards.
 270 No mortality was detected above 900 m (Fig. 6d). The elevational limit of tree mortality was
 271 negatively correlated with SPEI (Fig. 5).



272

273

Fig. 3. EVI and SPIE anomaly for the Kuznetzky Alatau Mountains and BI site. Box indicated BI location. (a) –

274

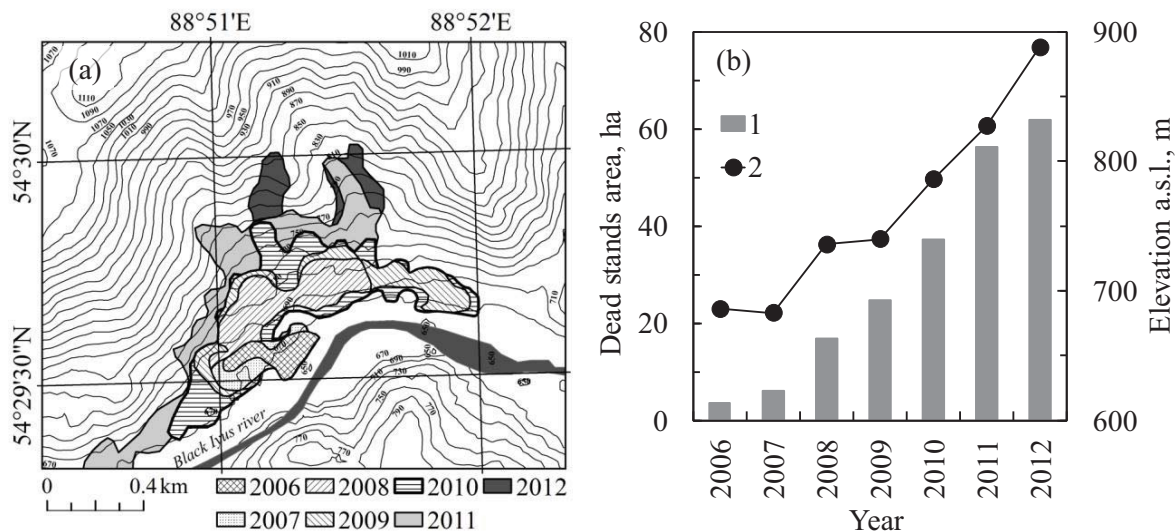
EVI anomaly (2012 vs 2000-2012 mean), (b) –SPEI anomaly (2000-2009 mean vs 1902-2009 mean), (c) – SPEI (1)

275

and EVI (2) dynamics for the BI site. Bars showed 0.95 confidence level. Trend are significant at $p < 0.007$ (EVI) and

276

at $p < 0.023$ (SPIE).



277

278

Fig. 4. (a) forest mortality map (background: a topo map) and (b) forest mortality dynamic (1 - dead stands area,

279

2 - elevation limit of dead stands at given year).

280

3.3. Dendrochronology data

281

The statistics of master-chronologies (both standard and residual) for “surviving” and “dead

282

and decline” groups are shown in Table 2. The mean tree ages of “survivors” and “dead and

283

decline” groups were 154 and 173 years, respectively. All groups have relatively high

284

correlations between individual series and master-chronology ($r^2 = 0.39-0.41$). Mean sensitivity

285

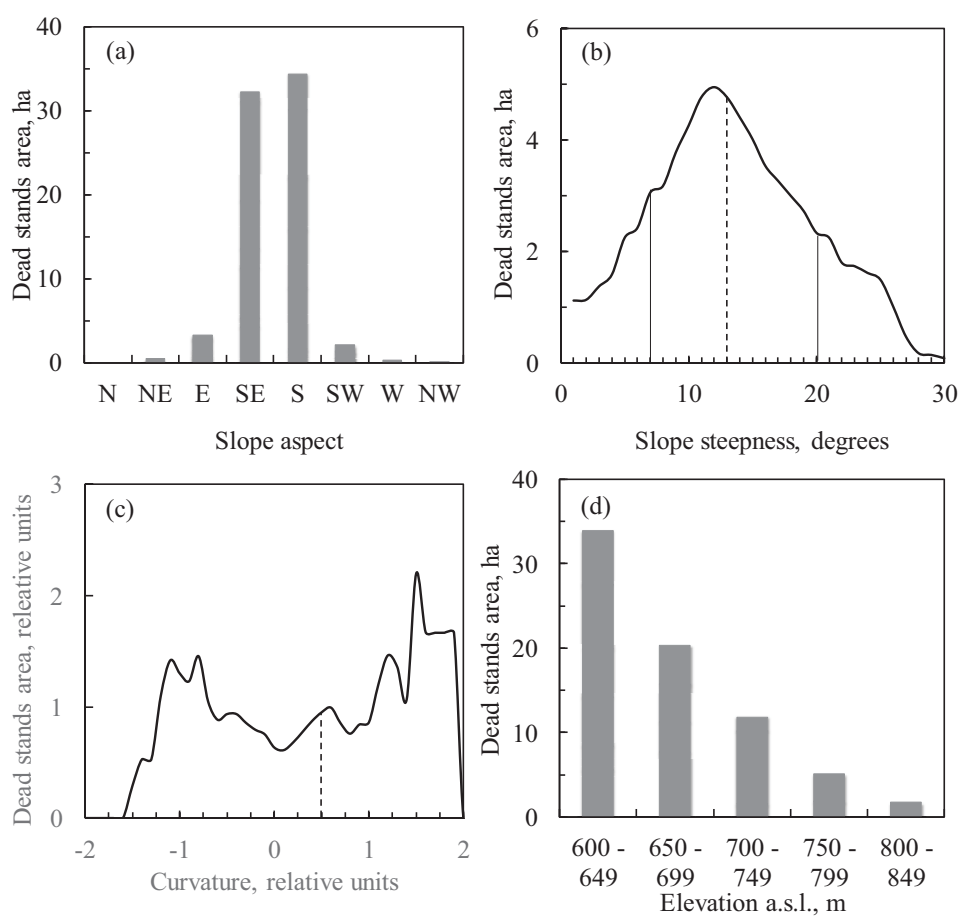
values which signify the relative change in ring-width from one year to the next, were low for all

286

Table 2. The tree-ring chronologies statistics

	Tree group		Master Chronology
	“Survivors”	“Dead & decline”	
Mean ring width (mm)	0.94	0.84	0.95
Maximum ring width (mm)	3.88	5.12	4.86
Mean sensitivity	0.180	0.183	0.173
Interseries correlation	0.39	0.41	0.43
Autocorrelation	0.69	0.63	0.60

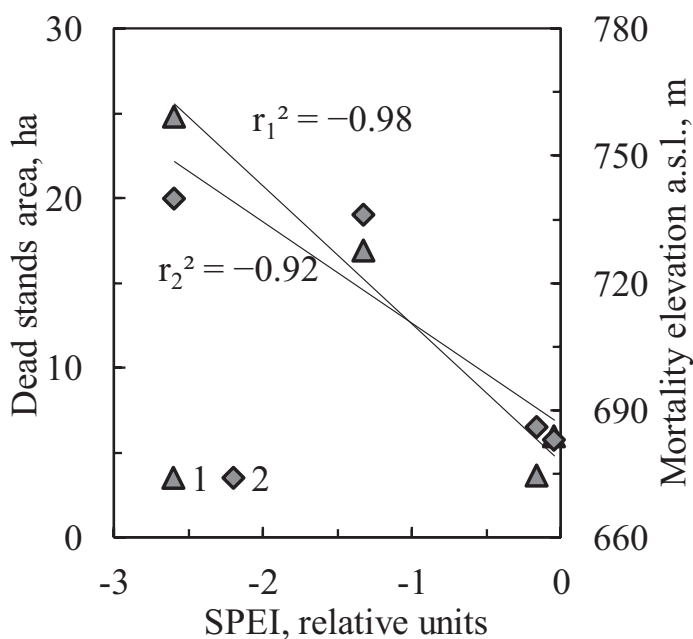
287



288

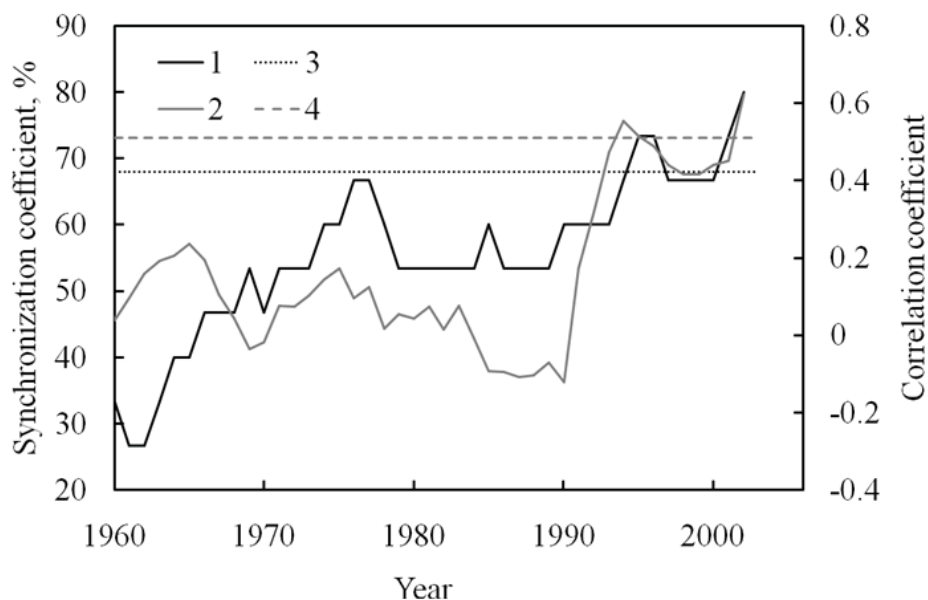
289 Fig. 5. Dynamics of forest mortality with respect to relief features. (a) - mortality dependence on aspect, (b) -
 290 mortality distribution with respect to slope steepness (dashed line: a median, thin lines: boundaries of 75% of dead
 291 stands area), (c) – mortality distribution on concave/convex relief features, (d) - mortality dependence on elevation.
 292 groups (0.180-0.183; i.e., the climate signal was low), which is indicative for trees with a
 293 favorable growth pattern (Shiyatov, 1986). Correlations for “survived” and “dead and decline”
 294 chronologies with master-chronology (0.92-0.97) were very high, i.e., trees growth pattern was
 295 homogeneous (Fritts, 1991).

296 No significant correlations were found between radial tree growth and temperature and
 297 precipitation. The relationship between tree radial growth and SPEI index was developed from
 298 correlations over the period from 1940 to 2009 yrs (with window sizes of 3, 5, 7, 9, 11 and 15
 299 yrs). To do this, a correlation was established between the first selected years of the climate
 300 record and the corresponding years for the tree-ring record. The same process was repeated with
 301 a 1-year lag through the end of the SPEI record. Similarly, a coefficient of synchronization was
 302 calculated. Tree radial increment was significantly correlated and synchronized with SPEI
 303 drought index ($r^2 = 0.37$, $r_s = 80$; Fig. 7). Trajectories of “dead” and “survivors” diverged at the
 304 beginning of the 21st century. Tree mortality was observed after the 1998 drought (Fig. 8).



305

306 Fig. 6. Dead stands area (1, r_1^2) and mortality elevation limit correlations with SPIE (2, r_2^2). r_1^2 and r_2^2 are
 307 significant at $p < 0.02$ and $p < 0.08$, correspondingly.



308

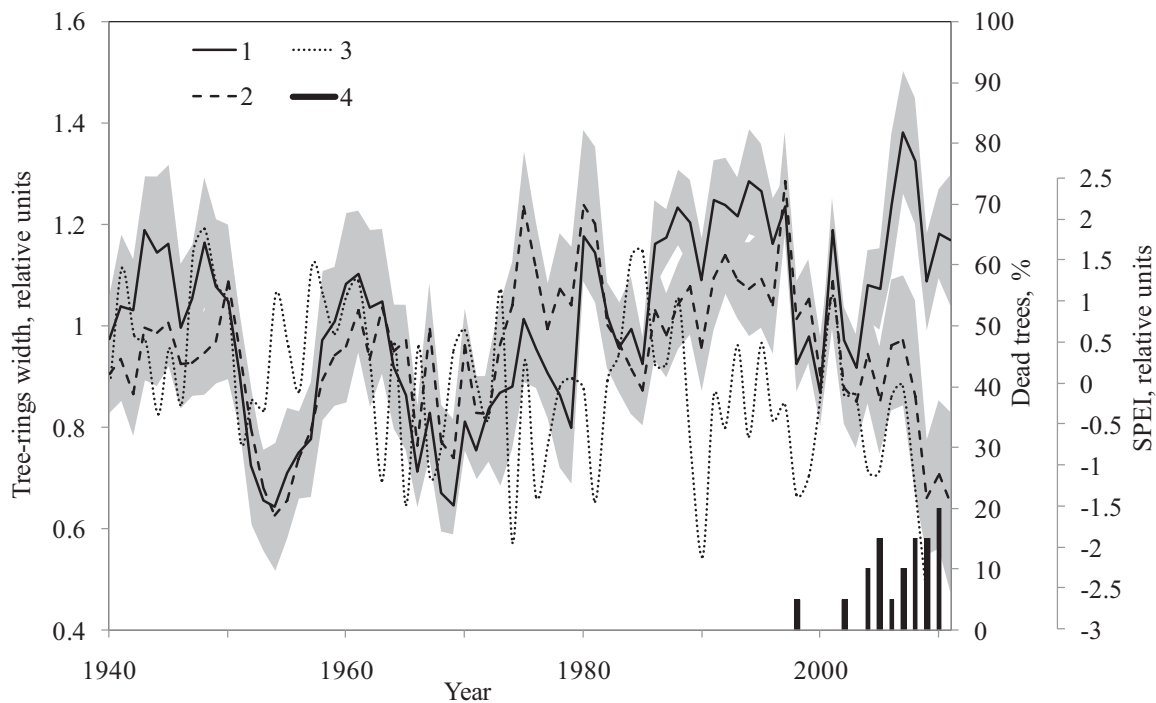
309

310

311

312

Fig. 7. Running 15-year coefficients of synchronization (1) and correlation (2) between tree ring radial growth SPIE and. 3 – level on medium (>69%) synchronization, 4 – significance level ($p > 0.05$) for correlation coefficients. Note: synchronization coefficient values $69 > r_s > 50$ were considered as a low, $r_s > 69$ were considered as a satisfactory (Shiyatov, 1986).



313

314

315

316

Fig. 8. Tree ring chronology of (1) “survivors” and (2) “dead and decline” trees. Confidence interval ($p < 0.05$) shown by grey background. 3 - SPEI dynamics, 4 – percentage of sampled dead trees ($n=21$) which dying in the given year.

317 4. Discussion

318 Siberian pine mortality was tracked since 2006, when mortality was first detectable (Fig.4a,
319 b). The spatial pattern of dead forest stands was uneven with respect to topographic relief
320 features. Dead stands were mainly located on slopes with southern aspect (Fig. 6b). This pattern
321 is typical for drought-induced mortality (e.g., aspen mortality in the western US (Huang and
322 Anderegg, 2012), or birch mortality in Trans-Baikal area, Russia (Kharuk et al., 2013). The area
323 of dead stands was correlated with a drought increase ($r_1^2 = 0.98$; Fig. 5).

324 The majority of dead stands were located on relatively steep slopes with the median at about
325 13° (Fig. 5c). The slope and aspect of those stands are approximately normal to peak direct solar
326 radiation during the middle of June to the beginning of July (when sun elevation angles reach
327 about 60°). Mortality was relatively higher within convex terrain elements (Fig. 5c), whereas
328 within areas of higher soil moisture (e.g., toeslopes and river alluvium terraces) mortality was
329 lower. These facts suggest moisture stress as a factor of forest mortality. The other evidence of
330 moisture stress impact is a strong correlation between mortality and drought index (Fig. 8).
331 Mortality was maximal within the lower elevation belt (starting from the footslope) and
332 decreased with elevation with no signs of mortality above 900 m (Fig. 4b). This elevational
333 pattern could be attributed to increased precipitation at higher elevations. Within the study area
334 precipitation increased with elevation by about 1.8 mm m^{-1} , which translates into 460 mm more
335 precipitation at 900 m in comparison with 650 m (i.e., where mortality was first observed; Fig.
336 4). As drought increased, mortality extended uphill and reached elevations of 900 m by the year
337 2012 (Fig. 6). The upward shift of mortality was correlated with SPEI values (Fig.5). It is
338 important to note that Siberian pine (which is also known as "tree-of-fog") is a precipitation-
339 sensitive species with optimal precipitation values $>1000 \text{ mm year}^{-1}$. At higher elevations (in
340 addition to precipitation increase) frequency of fogs (clouds) also increased. A drought impact
341 on Siberian pine was amplified by shallow well-drained soils especially at convex relief features.
342 Notably, less drought-sensitive birch and aspen trees, which make up about 1-3% of Siberian
343 pine stands, did not exhibit signs of drought impact.

344 Dendrochronology analysis also supported the hypothesis of the primary role of drought
345 stress in Siberian pine stands decline and mortality. Drought increase (Fig. 3b, c) was
346 accompanied by a decrease in radial increment (Fig. 7). Similar observations were reported for
347 aspen growth during drought years (Hogg et al., 2008). Starting at the end of the 20th century
348 trees increment trajectories diverged. The "decline and dead" group showed negative increment
349 trends, whereas "survivors" temporarily increased their growth increment (Fig. 7). The growth
350 release in the surviving trees was likely caused by a decrease in competition with the dying trees
351 since the surviving and declining trees were interspersed within the same stand. With drought

352 increase in the following years (2008-2009) radial increment of “survivors” also decreased
353 (Fig. 7).

354 Synchronization between tree radial growth and SPEI increased after 1960 and became
355 significant by the middle of the 1970s with highest values observed during the last decade (Fig.
356 7). Similarly, correlation between tree radial growth and SPEI was significant in the mid 1990s
357 and beginning of the 21st century and were increased by repeated extreme droughts during the
358 last decades (1998, 2003 and 2012 yrs; Fig. 7). This coincided with observations of other authors
359 of increased growth sensitivity to climate in the years preceding mortality (McDowell et al.,
360 2008). Increased synchrony between tree ring growth and SPEI also suggest that past droughts
361 narrowed the Siberian pine ecological niche. Thus, Siberian pine mortality occurred after
362 exposure to prior droughts (years 1998, 2002) that initiated tree ring growth decline (Fig. 8).
363 Similarly, aspen stands (*Populus tremuloides*) experienced severe stress in the beginning of the
364 21st century, which caused mortality of stands (Worrall et al., 2010; Anderegg, 2012).

365 The progressive decrease of tree increments (Fig. 8) indicated, along with water stress, the
366 presence of other effects (including possibly carbon starvation). Although in recent studies of
367 aspen die-off in western North America no evidence was found that drought stress led to
368 depletion of carbohydrate reserves (Anderegg et al., 2012). A potential (also secondary) role in
369 Siberian pine decline may be bark beetles attack. Thus, insect and larvae galleries were observed
370 within the bark and xylem of severely weakened and dead trees. It is known that bark beetles
371 attacked weak and old growth trees (e.g., Kharuk et al., 2004). However, this was not the case
372 within the study area where stands were not over mature (mean tree age was 160 years) and
373 Siberian pine stands become overmature at Age >300 yr. Evergreen conifer decline and mortality
374 in some Russian forests were also attributed to root fungi impacts, which were facilitated by a
375 drought-caused decrease in stand vigor (Chuprov, 2008; Pavlov et al., 2008). Fungi and insect
376 attacks should be considered as drought co-factors in the DNC decline phenomenon, which
377 agrees with conception of multiple mechanisms of drought-induced mortality (water stress,
378 carbohydrate depletion, and insect, fungi and bacterial attack) (McDowell et al., 2008;
379 McDowell, 2011; Anderegg et al., 2012; Choat et al., 2012; Fettig et al., 2013).

380

381 The problem of Siberian pine decline has a special significance for forest management,
382 because Siberian pine stands logging is strongly prohibited with the exception of declined stands.
383 In the last case, selective cutting is allowed. Thus legitimate forest harvesting is dependent on
384 timely management decisions based on forest monitoring data. Increasing climate impacted
385 Siberian pine mortality during recent decades and expected increase of precipitation-sensitive
386 species mortality point to the need for changes in forest management policy.

387 The studied site is within the marginal area between the forest-steppe and black taiga area,
388 and further increases in drought impacts may turn this area into forest-steppe. This will lead to,
389 in particular, introducing drought-resistant species (*Pinus silvestris*, *Larix sibirica*) via natural
390 succession. Meanwhile an expected decrease of the Siberian pine population in this area will not
391 require its assisted migration (as in the case of *Pinus albicaulis*; McLane and Aitken, 2012).
392 This species is not highly threatened by climate change because its area is (1) broad (from ca
393 49°N to 67°N) (2) there is evidence of climate-driven increase of Siberian pine area by its
394 invasion into larch habitat and into the alpine tundra zone (Kharuk et al., 2005, 2009).

395 Along the BI site, DNC within the Kuznetzky Alatau Mountains region experienced
396 increased drought (and vegetation index, EVI, decrease) during the end of the 20th - beginning of
397 the 21st centuries (Fig.3c). Several sites of tree decline and mortality were reported by local
398 foresters within these mountains and its vicinities (Fig. 1, sites 4).

399 On a broader scale, the Siberian pine stand mortality observed within the Kuznetzky
400 Alatau Mountains is part of the phenomenon of DNC decline and mortality in Siberia, European
401 Russia and Russian Far East. Forest mortality locations based on literature data and the authors'
402 observations are presented in Fig. 1. Notably all reported areas of DNC decline coincided with
403 the zones of negative SPEI values (i.e., drought increase; Fig. 1). Thus, monitoring of drought
404 severity (SPEI) is likely to be useful as an early warning indicator of climate-related mortality
405 across forests in other areas and regions, especially those composed of drought-sensitive species
406 (*Pinus sibirica*, *Abies sibirica* and *Picea obovata*). The data obtained are one of the first
407 observations of drought-induced decline and mortality of DNC at southern border of boreal
408 forests, and supported deforestation scenario within this zone with increasing aridity. Meanwhile
409 with an increase in aridity drought-resistant conifers (i.e., *Pinus silvestris* and *Larix sibirica*)
410 may replace DNC within its habitat. Drought increase may also slowdown Siberian pine
411 seedlings recruitment within the alpine forest-tundra ecotone at southern border of Siberian
412 forests (Kharuk et al., 2010a, 2010b).

413 This described phenomenon, along with published data on birch stands die-off in the Trans
414 Baikal zone (Kharuk et al., 2013), coincided with world-wide observations of increased episodes
415 of climate-induced forest decline and mortality (Aitken et al., 2008; Worrall et al., 2010;
416 Anderegg et al., 2012), and supports the hypothesis of wholesale redistribution of trees in the
417 next century (Aitken et al., 2008) . Thus, the extent, dynamics and causes of decline and
418 mortality in Siberian "dark needle conifer" forests warrants further investigation

419 **Acknowledgment**

420 This research was supported by the SB RAS Program No. 30.25 and NASA Science Mission
421 Directorate

422 **References**

- 423 Aitken, S.N., Yeaman, S., Holliday, J.A., Wang, T., Curtis-McLane, S., 2008. Adaptation,
424 migration or extirpation: Climate change outcomes for tree populations. *Evol. Appl.* 1(1),
425 95–111.
- 426 Allen, C.D., Macalady, A.K., Chenchouni, H., Bachelet, D., McDowell, N., Vennetier, M.,
427 Kitzberger, T., Rigling, A., Breshears, D.D., Hogg, E.H. (Ted), Gonzalez, P., Fensham, R.,
428 Zhang, Z., Castro, J., Demidova, N., Lim, J.H., Allard, G., Running, S.W., Semerci, A.,
429 Cobb, N., 2009. A global overview of drought and heat-induced tree mortality reveals
430 emerging climate change risks for forests. *For. Ecol. Manage.* 259(4), 660–684. doi:
431 10.1016/j.foreco.2009.09.001.
- 432 Anderegg, W.R.L., Berry, J.A., Smith, D.D., Sperry, J.S., Anderegg, L.D.L., Field, C.B., 2012.
433 The role of hydraulic and carbon stress in a widespread climate-induced forest die-off.
434 *Proc. Natl. Acad. Sci. U.S.A.* 109, 233–237.
- 435 Anderegg, W.R.L., 2012. Complex aspen forest carbon and root dynamics during drought.
436 *Clim. Change.* 111, 983–991. doi: 10.1007/s10584-012-0421-9.
- 437 Bartalev, S., Egorov, V., Ershov, D., Isaev, A., Loupian, E., Plotnikov, D., Uvarov, I., 2011.
438 Satellite mapping of the vegetation cover over Russia using MODIS spectroradiometer
439 data. *Contemporary Remote Sensing from the Space.* 8(4), 285–302. (In Russian).
- 440 Bigler, C., Braker, O.U., Bugmann, H., Dobbertin, M., Rigling, A., 2006. Drought as an inciting
441 mortality factor in Scots pine stands of the Valais, Switzerland. *Ecosystems.* 9, 330–343.
- 442 Breda, N., Huc, R., Granier, A., Dreyer, E., 2006. Temperate forest trees and stands under severe
443 drought: a review of ecophysiological responses, adaptation processes and long-term
444 consequences. *Ann. For. Sci.* 63, 625–644.
- 445 Breshears, D.D., Cobb, N.S., Rich, P.M., Price, K.P., Allen, C.D., Balice, R.G., Romme, W.H.,
446 Kastens, J.H., Floyd, M.L., Belnap, J., Anderson, J.J., Myers, O.B., Meyer, C.W., 2005.
447 Regional vegetation die-off in response to global-change-type drought. *Proc. Natl. Acad.*
448 *Sci. U.S.A.* 102 (42), 15144–15148.
- 449 Christensen, J.H., Hewitson, B., Busuioc, A., Chen, A., Gao, X., Held, I., Jones, R., Kolli, R.K.,
450 Kwon, W.-T., Laprise, R., Magan˜a Rueda, V., Mearns, L., Menerndez, C.G., Raisanen, J.,
451 Rinke, A., Sarr, A., Whetton, P., 2007. Regional climate projections. In: Solomon, S., et al.
452 (Eds.), *Climate Change: The Physical Science Basis. Contributions of Working Group I to*
453 *the Fourth Assessment Report of the Intergovernmental Panel on Climate Change.*
454 Cambridge University Press, Cambridge, United Kingdom/New York, NY.
- 455 Climate Explorer. <<http://climexp.knmi.nl>> (09.04.13).

- 456 Choat, B., Jansen, S., Brodribb, T.J., Cochard, H., Delzon, S., Bhaskar, R., Bucci, S.J., Field,
457 T.S., Gleason, S.M., Hacke, U.G., Jacobsen, A.L., Lens F., Maherali, H., Martínez-Vilalta,
458 J., Mayr, S., Mencuccini, M., Mitchell, P.J., Nardini, A., Pittermann, J., Pratt, R.B., Sperry,
459 J.S., Westoby, M., Wright, I.J., Zanne, A.E., 2012. Global convergence in the vulnerability
460 of forests to drought. *Nature*. 491, 752–755. doi:10.1038/nature11688.
- 461 Chuprov, N.P., 2008. Drying up of Spruce forests mortality within European Russia north. *Forest*
462 *management*. 1, 24–26. (In Russian).
- 463 Cook, E.R., Holmes, R. L., 1986. Chronology development, statistical analysis. Guide for
464 computer program ARSTAN. Laboratory of Tree Ring Research, the University of
465 Arizona. 1986, 50–65.
- 466 Dobbertin, M., Rigling, A., 2006. Pine mistletoe (*Viscum album ssp. austriacum*) contributes to
467 Scots pine (*Pinus sylvestris*) mortality in the Rhone valley of Switzerland. *For. Pathol.* 36,
468 309–322.
- 469 Efremov, D.F., Zakharenkov, A.S., Kopeikin, M.A., Kuzmichev, E.P. Smetanina, M.I.,
470 Soldatov, V.V., 2012. Forest Fire Prevention and Control in the Russian Forest
471 Management System. World Bank, Moscow.
- 472 Fettig, C.J., Reid, M.L., Bentz, B.J., Sevanto, S., Spittlehouse, D.L., Wang, T. 2013. Changing
473 climates, changing forests: A western North American perspective. *J. Forestry*, 111, 214-
474 228.
- 475 Fritts, H.C., 1991. Reconstruction Large-scale Climatic Patterns from Tree-Ring Data: A
476 Diagnostic Analysis. University of Arizona Press, Tucson.
- 477 Hansen, A.J., Nielson, R.P., Dale, V.H., Flather, C.H., Iverson, L.R., Currie, D.J., Shafer, S.,
478 Cook, R., Bartlein, P.J. 2001. Global change in forests: Responses of species,
479 communities and biomes. *Bioscience* 51: 765-779.
- 480 Hogg, E.H., Brandt, J.P., Michaellian, M., 2008. Impacts of a regional drought on the
481 productivity, dieback, and biomass of western Canadian aspen forests. *Canadian Journal of*
482 *Forest Research-Revue Canadienne De Recherche Forestiere*. 38, 1373–1384.
- 483 Holmes, R.L., 1983. Computer-assisted quality control in tree-ring dating and measurement.
484 *Tree-ring Bull.* 44, 69–75.
- 485 Huang, C.-Y., Anderegg, W.R.L., 2012. Large drought-induced aboveground live biomass losses
486 in southern Rocky Mountain aspen forests. *Glob. Chang. Biol.* 18, 1016–1027, doi:
487 10.1111/j.1365-2486.2011.02592.x.
- 488 Huete, A., Justice, C., van Leeuwen, W., 1999. MODIS vegetation index (MOD 13) - algorithm
489 theoretical basis document. <http://modis.gsfc.nasa.gov/data/atbd/atbd_mod14.pdf>
490 (09.04.13).

- 491 IPCC, 2007. Climate Change 2007: Synthesis Report. Valencia, Spain.
- 492 Kharuk, V.I., Ranson, K.J., Kozuhovskaya, A.G., Kondakov, Y.P., Pestunov, I.A., 2004.
- 493 NOAA/AVHRR satellite detection of Siberian silkmoth outbreaks in eastern Siberia, *Int. J.*
- 494 *Remote Sens.* 25(24), 5543-5555.
- 495 Kharuk, V.I., Dvinskaya, M.L., Ranson, K.J., Im, S.T., 2005. Expansion of evergreen conifers to
- 496 the larch-dominated zone and climatic trends. *Russian J. Ecol.* 36 (3), 164–170.
- 497 Kharuk, V.I., Ranson, K.J., Im, S.T., Dvinskaya, M.L., 2009. Response of *Pinus sibirica* and
- 498 *Larix sibirica* to climate change in southern Siberian alpine forest-tundra ecotone. *Scand. J.*
- 499 *For. Res.* 24(2), 130–139.
- 500 Kharuk, V.I., Im, S.T., Dvinskaya, M.L., Ranson, K.J., 2010a. Climate-Induced Mountain
- 501 Treeline Evolution in southern Siberia. *Scand. J. For. Res.* 25(5), 446–454.
- 502 Kharuk, V.I., Ranson, K.J., Im, S.T., Vdovin, A.S., 2010b. Spatial distribution and temporal
- 503 dynamics of high elevation forest stands in southern Siberia. *Glob. Ecol. Biogeogr.* 19,
- 504 822–830.
- 505 Kharuk, V.I., Ranson, K.J., Oskorbin, P.A., Im, S.T., Dvinskaya, M.L., 2013. Climate induced
- 506 birch mortality in trans-Baikal lake region, Siberia. *For. Ecol. Manage.* 289, 385–392.
- 507 Landmann, G., Dreyer, E. (Eds.), 2006. Special Issue: Impacts of drought and heat on forest.
- 508 Synthesis of available knowledge, with emphasis on the 2003 event in Europe. *Ann. For.*
- 509 *Sci.* 63(6), 567–652.
- 510 Lloyd, A.H., Bunn, A.G., 2007. Responses of the circumpolar boreal forest to 20th century
- 511 climate variability. *Environ. Res. Lett.* 2, 045013, doi:10.1088/1748-9326/2/4/045013.
- 512 Lucht, W., Schaphoff, S., Erbrecht, T., Heyder, U., Cramer, W., 2006. Terrestrial vegetation
- 513 redistribution and carbon balance under climate change. *Carbon Balance Manag.* 1(6).
- 514 doi:10.1186/1750-0680-1-6.
- 515 Man'ko, Yu.I., Gladkova, G.A., Butovets, G.N., Kamibayashi, N., 1998. An experience of
- 516 monitoring fir-spruce forest decline in the central Sikhote-Alin. *Russian J. Forestry.* 1, 3–
- 517 16. (In Russian).
- 518 McLane, S.C., Aitken, S.N., 2012. Whitebark pine (*Pinus albicaulis*) assisted migration
- 519 potential: testing establishment north of the species range. *Ecol. Appl.* 22(1), 142–153.
- 520 McDowell, N., Pockman, W.T., Allen, C.D., Breshears, D.D., Cobb, N., Kolb, T., Plaut, J.,
- 521 Sperry, J., West, A., Williams, D.G., Yezpez, E.A., 2008. Mechanisms of plant survival and
- 522 mortality during drought: why do some plants survive while others succumb to drought?
- 523 *New Phytol.* 178, 719–739.
- 524 McDowell, N.G., 2011. Mechanisms Linking Drought, Hydraulics, Carbon Metabolism, and
- 525 Vegetation Mortality. *Plant Physiol.* 155, 1051–1059.

- 526 Palmer, W.C., 1965. Meteorological droughts. U.S. Department of Commerce Weather Bureau
527 Research Paper. 45.
- 528 Pavlov, I.N., Ruhullaeva, O.V., Barabanova, O.A., Ageev, A.A., 2008. Estimation of root
529 pathogens impact on forest resources of Siberian federal district. Boreal zone conifers.
530 25(3-4), 262–268. (In Russian).
- 531 Pen˜uelas, J., Lloret, F., Montoya, R., 2001. Severe drought effects on Mediterranean woody
532 flora in Spain. For. Science. 47, 214–218.
- 533 Raffa, K.F., Aukema, B.H., Bentz, B.J., Carroll, A.L., Hicke, J.A., Turner, M.G., Romme, W.H.,
534 2008. Cross-scale drivers of natural disturbances prone to anthropogenic amplification: the
535 dynamics of bark beetle eruptions. BioScience. 58, 501–517.
- 536 Rinn, F., 1996. Tsap V 3.6. Reference manual: computer program for tree-ring analysis and
537 presentation. Heidelberg, Germany.
- 538 Sanitary and forest pathological state of forest resources in 2007 year, 2008. Rosleshoz report
539 <<http://www.rosleshoz.gov.ru/activity/pathology/reports/5>> (in Russian).
- 540 Shiyatov, S., 1986. Dendrochronology of upper timberline in Ural. Nauka, Moscow (in Russian).
- 541 Scholze, M., Knorr, W., Arnell, N.W., Prentice, I., 2006. A climate-change risk analysis for
542 world ecosystems. Proc. Natl. Acad. Sci. U.S.A. 103, 13116–13120.
- 543 Seager, R., Ting, M., Held, I., Kushnir, Y., Lu, J., Vecchi, G., Huang, H.-P., Harnik, N.,
544 Leetmaa, A., Lau, N.-C., Li, C., Velez, J., Naik, N., 2007. Model projections of an
545 imminent transition to a more arid climate in southwestern North America. Science. 316,
546 1181–1184.
- 547 StatSoft Inc., 2013. Electronic statistics textbook. Tulsa, OK.
548 <<http://www.statsoft.com/textbook>> (09.04.13).
- 549 Sterl, A., Severijns, C., Dijkstra, H., Hazeleger, W., van Oldenborgh, G.J., van den Broeke, M.,
550 Burgers, G., van den Hurk, B., van Leeuwen, P.J., van Velthoven, P., 2008. When can we
551 expect extremely high surface temperatures? Geophys. Res. Lett. 35, L14703
552 doi: 10.1029/2008GL034071.
- 553 Terra Norte. <<http://terranorte.iki.rssi.ru>> (05.05.12).
- 554 Van Mantgem, P.J., Stephenson, N.L., Byrne, J.C., Daniels, L.D., Franklin, J.F., Fuller, P.Z.,
555 Harmon, M.E., Larson, A.J., Smith, J.M., Taylor, A.H., Veblen, T.T., 2009. Widespread
556 increase of tree mortality rates in the western United States. Science. 323, 521–524.
- 557 Vicente-Serrano, S.M., Beguería, S., López-Moreno, J.I., 2010. A Multiscalar Drought Index
558 Sensitive to Global Warming. The Standardized Precipitation Evapotranspiration Index. J.
559 Climate. 23, 1696–1718. doi: 10.1175/2009JCLI2909.1.

560 Wang, D., Morton, D., Masek, J., Wu, A., Nagol, J., Xiong, X., Levy, R., Vermote, E., Wolfe,
 561 R., 2012. Impact of sensor degradation on the MODIS NDVI time series. *Remote Sens.*
 562 *Environ.* 119, 55–61, doi: 10.1016/j.rse.2011.12.001

563 Worrall, J.J., Marchetti, S.B., Egeland, L., Mask, R.A., Eager, T., Howell, B., 2010. Effects and
 564 etiology of sudden aspen decline in southwestern Colorado, USA. *For. Ecol. Manage.*
 565 260(5), 638-648. doi:10.1016/j.foreco.2010.05.020.

566 **Figure captions**

567

568 Fig. 1. Location of known forest stands decline and mortality in Siberia. Background: evergreen
 569 conifer map (Bartalev et al., 2011). Color scale: SPEI (Standard Precipitation Evaporation Index)
 570 anomaly (2000-2009 vs 1902-2009.). Sites: 1 – spruce stands in Archangelsk region; 2 – DNC of
 571 Kuznetzky Alatau Mountains (location of this study designated by the red box); 3, 4 – DNC
 572 stands in southern Siberia; 5 – fir and Siberian pine site in southern Baikal area; 6 – birch stands
 573 within Trans-Baikal area (Kharuk et al., 2013); 7 – spruce and fir stands in Russian Far East
 574 (Man'ko et al., 1998).

575

576 Fig.2. Climate variables within “Black Iyus” site. (a), (b) – mean air temperature and
 577 precipitation anomalies, correspondingly (1 – annual; 2 – May-August data); (c) – anomaly of
 578 SPEI drought index; (d) – annual (1) temperature and (2) precipitation. Trends for annual
 579 temperature (a) and SPEI (c) were significant at $p < 0.05$. Data were averaged for a cell size
 580 $0.5^\circ \times 0.5^\circ$.

581

582 Fig.3. EVI and SPEI anomaly for the Kuznetzky Alatau Mountains and BI site. Box indicates
 583 location of the BI study area. (a) – EVI anomaly (2012 vs 2000-2012 mean); (b) – SPEI anomaly
 584 (2000-2009 mean vs 1902-2009 mean); c) – EVI (1) and SPEI (2) dynamics for the BI site. Bars
 585 show 0.95 confidence level. Trends are significant at $p < 0.007$ (EVI) and at $p < 0.023$ (SPEI).

586

587 Fig.4. (a) Forest mortality map (background: topographic map) and (b) trend of forest mortality
 588 from 2006 to 2012 (1 – dead stands area; 2 – elevation limit of dead stands at given year).

589

590 Fig. 5. Dead stands area (1, r_1^2) and mortality elevation limit correlations with SPEI (2, r_2^2).
 591 3, 4 – linear regressions of the dead stands area and mortality elevation limit, correspondingly.
 592 r_1^2 and r_2^2 are significant at $p < 0.02$ and $p < 0.08$, respectively.

593

594 Fig.6. Characteristics of forest mortality with respect to relief features. (a) – Mortality
595 dependence on aspect; (b) – mortality distribution with respect to slope steepness (dashed line: a
596 median, thin lines: boundaries of 75% of dead stands area); (c) – mortality distribution on
597 concave/convex relief features; (d) – mortality dependence on elevation.

598

599 Fig.7. Running 15-year coefficients of synchronization (1) and correlation (2) between tree ring
600 radial growth and SPEI; (3) – level of medium (>69%) synchronization; 4 – significance level
601 ($p>0.05$) of correlation coefficients. Note: synchronization coefficient values $69>r_s>50$ were
602 considered as a low, $r_s>69$ were considered as a satisfactory (Shiyatov, 1986).

603

604 Fig.8. Tree ring chronology of (1) “survivors” and (2) “dead and declining” trees. Confidence
605 interval ($p<0.05$) shown by gray background; 3 – SPEI dynamics; 4 – percentage of sampled
606 dead trees ($n=21$) which died in the given year.

607